Available online at www.sciencedirect.com

ScienceDirect

Ceramics International 38S (2012) S453–S456

CERAMICS
INTERNATIONAL

www.elsevier.com/locate/ceramint

Synthesis and characterization of Pt nanoparticles assembled in poly(3,4-ethylenedioxythiophene):polystyrene sulfonate

Seok-Joo Wang, Yong-June Choi, Hyung-Ho Park [*]

Department of Materials Science and Engineering, Yonsei University, Seoul 120-749, Republic of Korea

Abstract

Conducting poly(3,4-ethylenedioxythiophene):polystyrene sulfonate (PEDOT:PSS) composites containing Pt nanoparticles were synthesized by one-step method. Pt nanoparticles were formed in commercial PEDOT:PSS solution by hydrothermal reaction, alcohol reduction, and electron exchange with PEDOT and stabilized by PSS $[PtCl_6]^{2-}$ ions reduced completely after 4 h and Pt nanoparticles of arbitrary diameter in the range 3.0–5.0 nm were obtained. Considering refluxing time, slightly increased and narrow-sized Pt nanoparticles were stabilized and immobilized in the conducting polymer, PEDOT:PSS matrix. The formation and growth of Pt nanoparticles were characterized by using X-ray diffractometer, transmission electron microscopy, X-ray absorption spectroscopy, and X-ray photoelectron spectroscopy. Furthermore the electrostatic or chemical interaction between Pt nanoparticles and PSS^- chain was also confirmed.

Keywords: A. Films; A. Mixing; B. Spectroscopy; E. Functional applications

1. Introduction

Nanocomposites of conjugated polymers and inorganic particles have received much attention. Conjugated polymers have great advantages due to their high electrical conductivity and redox properties, and extensive applications ranging from batteries to light emitting devices have been carried out [1,2]. Many inorganic particles have been encapsulated in conjugated polymers. Such nanocomposites showed various interesting characteristics, particularly in the study of dielectric properties, energy storage, catalytic activity, and magnetic susceptibility [3,4]. The electronic structure of polymer chain can be strongly influenced by the characteristics of embedded metal nanoparticles [5,6]. These potentialities are due to a high specific surface area and the quantum size effect, which is derived from the dramatic reduction of the number of free electrons in particles in the range of 1–10 nm [7]. Needless to say, an accurate control of the particle size and distribution is the most important to investigate those unique physical and chemical properties.

Han et al. [8] have reported that the reduced forms of polypyrrole and polyaniline were converted to the respective oxidized forms with simultaneous in situ reduction of metal ions Au (III) to their elemental form, which, however, was not dispersed in most common solvents. We believe that stable colloidal forms of nanocomposites consisting of metal nanoparticles protected with conjugated polymer would provide various interesting characteristics and new features in nanotechnology applications [9–11].

In this study, conducting PEDOT:PSS film containing Pt nanoparticles were obtained in one step without an additional stabilizer for Pt nanoparticles. Through the reduction of $H_2PtCl_6{\cdot}xH_2O$ by hydrothermal reaction, conjugated polymer led to Pt nanoparticles with narrow size distribution and protected Pt nanoparticles as a stable form. This paper describes the synthesis and characterization of Pt nanoparticles protected with conjugated PEDOT:PSS.

2. Experimental

PEDOT:PSS (Baytron AI 4083) was purchased from HC stark. Hexachloroplatinic acid hexahydrate ($H_2PtCl_6{\cdot}xH_2O$, Aldrich Co.) was used as purchased. Iso-propanol was guaranteed grade and used without further purification. In a

---

[*] Corresponding author. Tel.: +82 2 21232853; fax: +82 2 3125375.
E-mail address: hhpark@yonsei.ac.kr (H.-H. Park).

0272-8842/$36.00 © 2011 Elsevier Ltd and Techna Group S.r.l. All rights reserved.
doi:10.1016/j.ceramint.2011.05.038

typical reaction, 0.001 g of $H_2PtCl_6{\cdot}xH_2O$ was dissolved in 0.5 ml of isopropyl alcohol and added to 1 ml of aqueous solution of PEDOT:PSS. Reaction took place at 60 °C under magnetic stirring for 1–24 h and PEDOT:PSS nanocomposite films containing Pt nanoparticles were prepared by spin casting at 500 rpm. The films were annealed for 15 min at each stepwise temperature of 80, 120, and finally 230 °C.

To examine the crystalline structure of Pt nanoparticles, X-ray diffraction (XRD) experiment was performed at 8C1 beamline of Pohang Accelerator Laboratory (PAL) in Pohang, Korea. We set the energy of incident X-rays as conventional Cu Kα energy (8.05 keV, $\lambda = 0.15425$ nm). Transmission electron microscopy (TEM) measurement was conducted at 200 kV on a Hitachi H-7100 electron microscope. We used the PAL 3C1 beamline to X-ray absorption spectroscopy (XAS) experiment. XAS was measured around Pt L_{III} edge (11.564 keV). Experiments were done with the fluorescence mode and the X-ray energy resolution was $\Delta E/E = 2 \times 10^{-4}$. The position of double crystal monochromator was calibrated by the standard Pt-foil. X-ray photoelectron spectroscopy (XPS) measurements were carried out on ESCALAB 220-*i*XL (VG scientific) using Al Kα (1486.6 eV) radiation to examine electronic interaction between PEDOT:PSS and Pt nanoparticles during the formation of PEDOT:PSS–Pt hybrid system.

3. Results and discussion

Pt nanoparticles were prepared in conjugate polymer PEDOT:PSS by one step reaction and three successive mechanism could be considered. PEDOT:PSS is highly acidic aqueous solution as for alcohol reduction and sonochemical reaction. Moreover, electrostatic bonded PEDOT:PSS provides electron exchange and stabilized site for Pt nanoparticles during solution reflux. As the refluxing time increase, reduction of $[PtCl_6]^{2-}$ salt ions, Pt^+ ions, and Pt–OH without surfactant is probable according to the hydrothermal reaction ($H_2PtCl_6{\cdot}xH_2O + 2RCH_2OH \rightarrow Pt^0 + 2RCHO + 6HCl + xH_2O$; $H_2PtCl_6 + 2H_2 \rightarrow Pt^0 + 6HCl$), alcohol reduction ($Pt{-}OH + H^+ + e^- \rightarrow Pt^0 + H_2O$), and electron exchange with polymer ($Pt^+ + PEDOT^0 \rightarrow Pt^0 + PEDOT^+$).

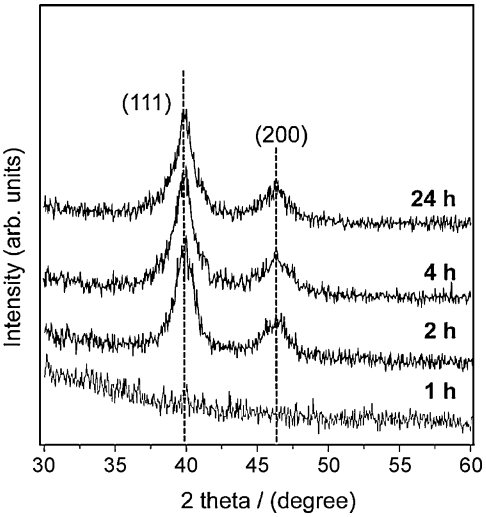

Fig. 1. X-ray diffraction patterns of Pt nanoparticles prepared in PEDOT:PSS with various refluxing time (1, 2, 4, and 24 h).

Fig. 1 shows XRD patterns of nanoparticles prepared in PEDOT:PSS with various refluxing time. The diffraction peaks of (1 1 1) and (2 0 0) from Pt with face centered cubic structure are clearly recognizable. Broad diffraction peaks indicate the small particle size as 4.2 ± 0.3, 4.3 ± 0.3, and 4.9 ± 0.3 nm with refluxing time of 2, 4, and 24 h, respectively by using the Scherrer equation [12]. High resolution TEM studies of the samples allowed us to clearly identify the Pt nanoparticles in the PEDOT:PSS polymer. After 4 h of refluxing time, uniform spherical aggregates of Pt nanoparticles could be synthesized within PEDOT:PSS solution without any stabilizing agent, such as sodium dodecyl sulfate (SDS) in Fig. 2. In Fig. 2(a), Pt nanoparticles were roughly spherical in shape with uniform size

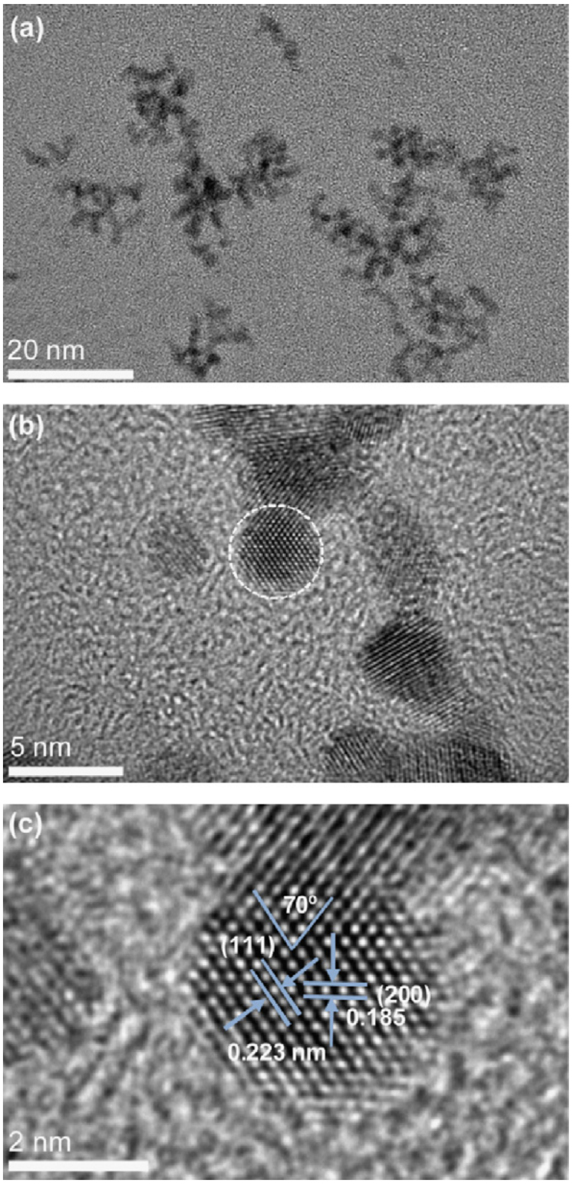

Fig. 2. TEM image and its high resolution images of Pt nanoparticles in PEDOT:PSS with refluxing time of 4 h.

of 2–4 nm. The TEM micrographs of single crystalline Pt nanoparticle (Fig. 2(b and c)) showed the fringe pattern of crystalline planes of Pt (2 0 0) and (1 1 1) with interplanar spacing of 0.185 and 0.223 nm, respectively.

In the following, XANES was applied to investigate the structural change of Pt nanoparticles under different reaction time in PEDOT:PSS solution. Fig. 3 shows the Pt L_{III}-edge XANES spectra of Pt foil, $H_2PtCl_6 \cdot xH_2O$ and Pt nanoparticles in PEDOT:PSS system. The absorption intensity was given in arbitrary unit. In the edge position of normalized absorption intensity, there was a change in the absorption intensity and edge position of Pt nanoparticles with different refluxing time as compared to the standard reference spectra of Pt foil (bottom) and $H_2PtCl_6 \cdot xH_2O$ (top). The maximum intensity was reduced and shifted to lower excitation energy with increased refluxing time. These tendencies in the spectra showed that metallic Pt nanoparticles showed intermediate behavior between $H_2PtCl_6 \cdot xH_2O$ and Pt foil. These data can be considered that $[PtCl_6]^{2-}$, PtOH and PtO (Pt^{2+} oxidation state) are gradually reduced to Pt (metallic) to form Pt nanoparticle [13]. L_{III}-edge showed clearer and larger decrease of hybridized anti-bonding orbital between 2p-orbital of oxygen (or 3d-orbital of chlorine) and 5d orbital of Pt with refluxing time, and this reduction might be corresponded to the formation and growth of Pt nanoparticles. The absorption energies after 4 h refluxing were shifted to smaller photon energy: more metallic state of Pt [14]. A decrease and broadening of post edge peak around 11577 eV corresponding to the hybridization of d-photoelectron state with localized chlorine 3d state was observed with fluxing time [14]. It was also confirmed by the disappearance of Cl 2p core level peak in XPS analysis.

A gradual generation of metallic Pt nanoparticles from $H_2PtCl_6 \cdot xH_2O$ with refluxing time was also monitored with XPS. In Fig. 4(a) of Pt 4f photoelectron spectra, a gradual decrease of peak binding energy of Pt 4f was observed. It was reported that the Pt $4f_{7/2}$ and $4f_{5/2}$ peak binding energies for Pt foil (typically metallic Pt state) are observed at 71.3 and 74.7 eV [15]. Through a decomposition of Pt 4f peak obtained from the 4 h refluxing sample (Fig. 4(b)), the presence of a small population of Pt–δ or Pt–OH was confirmed from the Pf $4f_{7/2}$ at 73.1 eV. Furthermore it was found that $4f_{7/2}$ and $4f_{5/2}$ peak binding energies of the Pt nanoparticles were shifted to high binding energy of 71.8 and 75.1 eV, respectively. From the comparison with the XANES data, this binding energy shift for Pt nanoparticles with refluxing time indicates the electrostatic or chemical interaction between Pt nanoparticles and PSS^- chain.

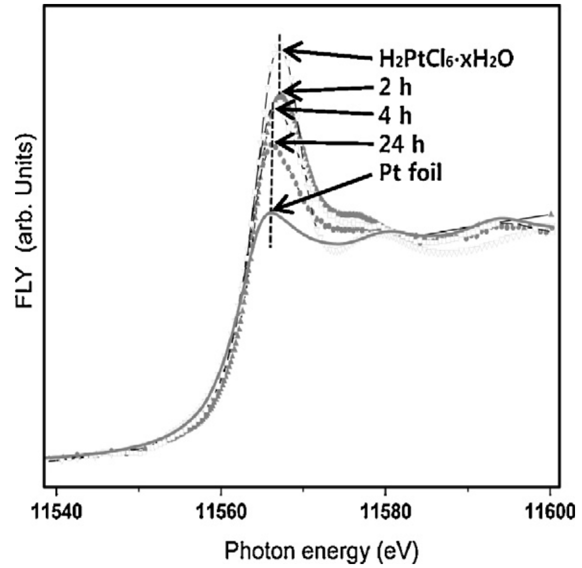

Fig. 3. Pt L_{III} XANES spectra of Pt reference foil, $H_2PtCl_6 \cdot 2H_2O$, and Pt nanoparticles after cross-linking with PEDOT:PSS with various refluxing time (2, 4, and 24 h). Measurements were performed at PAL 3C1 (The arrows point out the maximum intensity position of each spectrum).

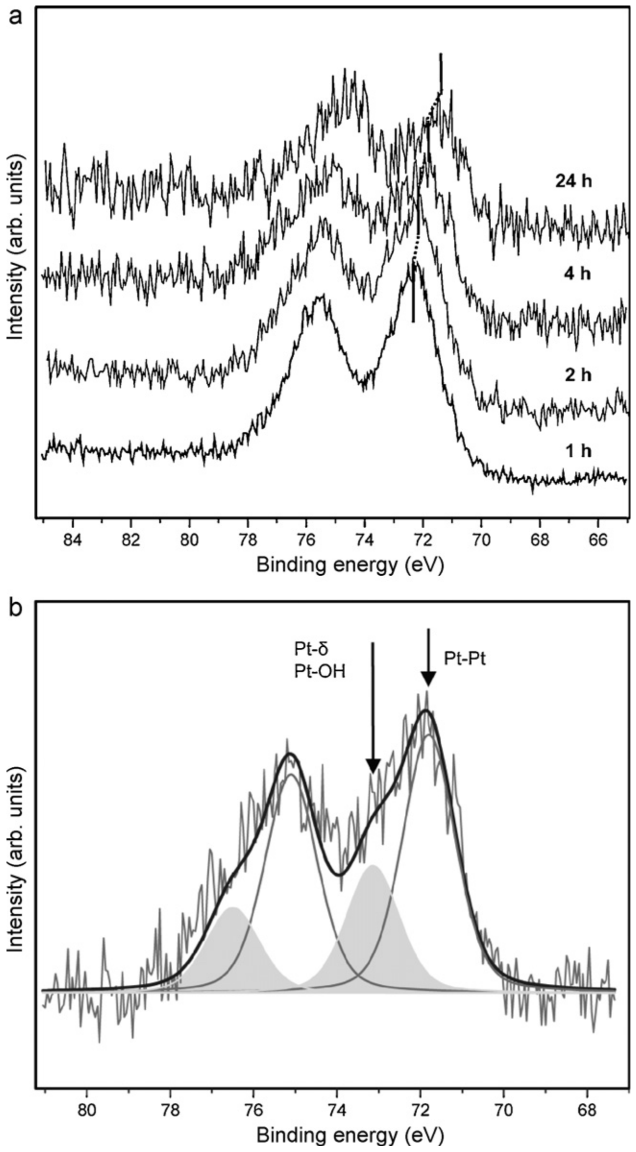

Fig. 4. X-ray photoelectron spectra of Pt nanoparticles prepared in PEDOT:PSS solution showing the Pt 4f region with the fitting results (using Shirley type background).

4. Conclusions

In summary, we synthesized Pt nanoparticles by one step through the variation of refluxing time using PEDOT:PSS solution without any strong reagent of $NaBH_4$ or organic surfactant of SDS. Pt nanoparticles were uniform in size of 2–4 nm. Decomposition of $H_2PtCl_6{\cdot}xH_2O$ to Pt^0 was completed after 4 h of refluxing and the generated Pt nanoparticles would provide large surface area for further nucleation and growth with increased refluxing time. All these developments without using any additives would improve the application and performance of Pt nanoparticle-conducting polymer composite in many industrial applications.

Acknowledgements

This research was supported by Future-based Technology Development Program (Nano Fields) through the National Research Foundation of Korea (NRF) funded by the Ministry of Education, Science and Technology (2009-0082604). Experiments at PLS were supported in part by MEST and POSTECH.

References

[1] A. Kraft, A.C. Grimsdale, A.B. Holmes, Elektrolumineszierende konjugierte polymere-polymere erstrahlen in neuem licht, Angewandte Chemie 110 (1998) 416–443.

[2] G. Horowitz, Organic field-effect transistors, Advanced Materials 10 (1998) 365–377.

[3] J.A. Smith, M. Josowicz, J. Janata, Polyaniline–gold nanocomposite system, Journal of The Electrochemical Society 150 (2003) E384–E388.

[4] S. Tian, J. Liu, T. Zhu, W. Knoll, Polyaniline/gold nanoparticle multilayer films: assembly, properties, and biological applications, Chemistry of Materials 16 (2004) 4103–4108.

[5] V.L Colvin, M.C. Schlamp, A.P. Alivisatos, Light-emitting diodes made from cadmium selenide nanocrystals and a semiconducting polymer, Nature 370 (1994) 354–357.

[6] C.J. Murphy, Nanocubes and nanoboxes, Science 298 (2002) 2139–2141.

[7] W.P. Halperin, Quantum size effects in metal particles, Reviews of Modern Physics 58 (1986) 533–606.

[8] M.Y. Han, C.H. Quek, W. Huang, C.H. Chew, L.M. Gan, A simple and effective chemical route for the preparation of uniform nonaqueous gold colloids, Chemistry of Materials 11 (1999) 1144–1147.

[9] Y. Zhou, H. Itoh, T. Uemura, K. Naka, Y. Chujo, Synthesis of novel stable nanometer-sized metal (M = Pd, Au, Pt) colloids protected by a π-conjugated polymer, Langmuir 18 (2002) 277–283.

[10] A.V. Kukhta, E.E. Kolesnik, A.I. Lesnikovich, M.N. Nichik, A.N. Kudlash, S.A. Vorobyova, Organic–inorganic nanocomposites: optical and electrophysical properties, Synthesis and Reactivity in Inorganic, Metal-Organic Chemistry, and Nano-Metal Chemistry 37 (2007) 333–339.

[11] C. Ingrosso, A. Panniello, R. Comparelli, M.L. Curri, M. Striccoli, Colloidal inorganic nanocrystal based nanocomposites: functional materials for micro and nanofabrication, Materials 3 (2010) 1316–1352.

[12] Y. Qi, T. Çağın, Y. Kimura, W.A. Goddard III, Molecular-dynamics simulations of glass formation and crystallization in binary liquid metals: Cu–Ag and Cu–Ni, Physical Review B 59 (1999) 3527–3533.

[13] Y. Gauthier, R. Baudoing-Savois, J.M. Bugnard, W. Hebenstreit, M. Schmid, P. Varga, Segregation and chemical ordering in the surface layers of $Pt_{25}Co_{75}$(1 1 1): a LEED/STM study, Surface Science 466 (2000) 155–166.

[14] A.L. Ankudinov, J.J. Rehr, J.J. Low, S.R. Bare, Theoretical interpretation of XAFS and XANES in Pt clusters, Topics in Catalysis 18 (2002) 3–7.

[15] J.E. Drawdy, G.B. Hoflund, S.D. Gardner, E. Yngvadottir, D.R. Schryer, Effect of pretreatment on a platinized tin oxide catalyst used for low-temperature Co oxidation, Surface and Interface Analysis 16 (1990) 369–374.